HHS Public Access

Author manuscript

Angew Chem Int Ed Engl. Author manuscript; available in PMC 2018 June 06.

Published in final edited form as:

Angew Chem Int Ed Engl. 2017 June 06; 56(24): 6921–6926. doi:10.1002/anie.201703244.

N_2-to-NH_3 Conversion by a triphos–Iron Catalyst and Enhanced Turnover under Photolysis

Trixia M. Buscagan, **Dr. Paul H. Oyala**, and **Prof. Jonas C. Peters***

Division of Chemistry and Chemical Engineering, California Institute of Technology, 78457 1200 E California Blvd, Pasadena CA 91103 (USA)

Abstract

Bridging iron hydrides are proposed to form at the active site of MoFe-nitrogenase during catalytic dinitrogen reduction to ammonia and may be key in the binding and activation of N_2 via reductive elimination of H_2. This possibility inspires the investigation of well-defined molecular iron hydrides as precursors for catalytic N_2-to-NH_3 conversion. Herein, we describe the synthesis and characterization of new $P_2^{P'Ph}Fe(N_2)(H)_x$ systems that are active for catalytic N_2-to-NH_3 conversion. Most interestingly, we show that the yields of ammonia can be significantly increased if the catalysis is performed in the presence of mercury lamp irradiation. Evidence is provided to suggest that photo-elimination of H_2 is one means by which the enhanced activity may arise.

Graphical abstract

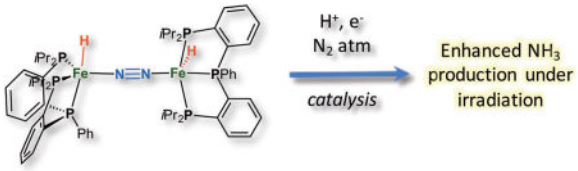

Light it up: Light-enhanced N_2-to-NH_3 conversion catalysis is reported. New triphos-supported $Fe(N_2)H_x$ catalysts provide higher ammonia yields for 1 atm N_2, and as much as 180% improvement upon irradiation by a mercury lamp.

Keywords

ammonia; hydrides; iron complexes; nitrogen fixation; photolysis

Biological nitrogen reduction is catalyzed by nitrogenase enzymes, and the active site of the most well-studied MoFe-nitrogenase, the FeMo-cofactor (FeMoco), contains seven iron centers and one molybdenum center (Figure 1, top).[1–3] Interest in understanding the mechanisms of biological nitrogen fixation has inspired many biochemical,[4–6]

* jpeters@caltech.edu.

Supporting information and the ORCID identification number(s) for the author(s) of this article can be found under: https://doi.org/10.1002/anie.201703244.

Conflict of interest

The authors declare no conflict of interest.

spectroscopic,[7,8] theoretical,[9] and synthetic model studies.[10–20] While a wealth of insight has been gained, a detailed atomic level understanding of biological nitrogen fixation is yet to be resolved.

Iron is the only metal present in all three of the known nitrogenases (MoFe-, VFe-, FeFe-N_2ase) and heterogeneous iron catalysts are among the most common in the industrial Haber–Bosch process.[22] These facts have motivated our group and others to develop single (or multiple) site Fe complexes that can bind and activate dinitrogen.[15, 17, 18, 23–27] To this end, we have reported the catalytic reduction of nitrogen to ammonia using Fe complexes supported by a tetradentate P_3^E ligand scaffold (E = B, C, or Si).[17, 20, 28–32] Using the P_3^BFe catalyst, significant turnover to generate NH_3 has been demonstrated.[20, 32] Other Fe systems supported by carbene and phosphine ligands have also shown efficacy for catalytic N_2-to-NH_3 conversion in recent reports.[15, 18] Freeze-quenched ^{57}Fe Mössbauer spectroscopic studies of a catalytic reaction using our P_3^BFe$(N_2)^-$ system have shown that a significant amount of the iron is tied up as an iron hydride–borohydride complex, $(P_3^B)(\mu\text{-}H)Fe(N_2)(H)$, believed to be an off-path state of the system;[20] this species can presumably convert back into an on-path $P_3^B Fe(N_2)^{\{0,-1\}}$ species via formal H_2 loss under turnover conditions.

Bridging hydride ligands have been proposed to accumulate at the FeMoco under turnover conditions (“E_4(4 H) state”; Figure 1, bottom) and may be key in the binding and activation of N_2 via reductive elimination of H_2.[3, 21, 33, 34, 35a] Recently, photochemically induced loss of H_2 from a presumed E_4 state of the FeMoco has been suggested.[35] The likelihood that M–H species may serve as common intermediates and/or side products of catalytic nitrogen fixation[21] motivates further studies of iron hydrides using well-defined molecular systems that fix N_2. In this latter context, molecular $Fe(H)_x$ complexes bearing terminal hydride ligands have been reported to undergo photosubstitution of N_2 with concomitant release of H_2 (Scheme 1).[36–38] Furthermore, $Fe(H)_x$ (x = 2 or 3) complexes are known that readily lose H_2 upon exposure to N_2.[36, 39, 40]

To expand the structural diversity of synthetic iron hydride catalysts capable of catalytic N_2-to-NH_3 conversion,[15, 17, 18, 20] we targeted a triphosphine ligand that supports reactive $Fe(N_2)(H)_x$ fragments. Herein, we report the synthesis of a dinuclear $[Fe^I(H)]_2(\mu\text{-}N_2)$ complex supported by a trisphosphine ligand, $P_2^{P'Ph}$ (Figure 2), that is a catalyst for N_2-to-NH_3 conversion in the presence of $[H(OEt_2)_2][BAr^F{}_4]$ ($HBAr^F{}_4$, $BAr^F{}_4$ = tetrakis(3,5-bis(trifluoromethyl)phenyl)-borate) and potassium graphite (KC_8). Of primary interest is that significantly enhanced ammonia yields (as much as 180% increase) are observed under Hg lamp irradiation. Based on this observation, we also examine the previously reported, P_3^BFe$(N_2)^-$ catalyst system (Figure 2)[17, 20] and show that it too gives significantly higher catalytic turnover (by ca. 50%) under Hg lamp photolysis.

$P_2^{P'Ph}$ (**1**) was synthesized by the addition of phenyl Grignard to the known bis(*o*-diisopropylphosphino-phenyl)-chlorophosphine[41] and exhibits two overlapping doublets centered at $\delta = -2.2$ ppm and two overlapping triplets at $\delta = -14.3$ ppm by ^{31}P NMR spectroscopy, suggesting a mixture of rotamers. Complexation of **1** with one equivalent of $FeBr_2$ yielded paramagnetic $P_2^{P'Ph}FeBr_2$ **2** as a purple-black crystalline solid (87% yield,

Scheme 2). The solid-state structure of **2-FeBr$_2$** shows a distorted trigonal bipyramidal geometry at iron with τ_5 = 0.54 (see the Supporting Information).[42] The solution magnetism of **2-FeBr$_2$** indicates spin equilibria, with solution magnetic moments of 3.40 μ_B at 200 K and 4.29 μ_B at 328 K. The $^{57}FeCl_2$ complex (**2-^{57}FeCl$_2$**) was analogously synthesized and exhibits similar solution magnetism (see the Supporting Information). The solid-state Mössbauer spectrum of the $^{57}FeCl_2$ complex was collected and gives rise to two quadrupole doublets, a minor S = 2 species (δ = 0.85 mm s^{-1} and ΔE_Q = 2.74 mm s^{-1}) and a major S = 1 component (δ = 0.53 mm s^{-1} and ΔE_Q = 0.62 mm s^{-1}).

Treatment of **2-FeBr$_2$** with two equivalents of NaHBEt$_3$ in THF at low temperature under an N_2 atmosphere provided the diamagnetic diiron(I) species [$P_2^{P'Ph}$Fe(H)]$_2$(μ-N_2) **3** as a green-black crystalline solid (64% yield, Scheme 2). The solid-state structure of **3** shows end-on N_2 binding between the two iron centers (N–N distance of 1.15 Å; Figure 3a). While the hydride ligands (one hydride ligand per Fe center) could not be located in the Fourier difference map, their presence was confirmed by IR spectroscopy. The Fe-D analogue, **3-D**, was synthesized using LiDBEt$_3$ in toluene. Infrared spectra of solid **3** and **3-D** exhibit expected peak shifts in the Fe–H(D) vibrations from 1833 and 1734 cm^{-1} for **3** to 1324 cm^{-1} and 1256 cm^{-1} for **3-D** (see the Supporting Information), consistent with the predicted values calculated from a simple harmonic oscillator model (1309 cm^{-1} and 1237 cm^{-1}). While **3** does not feature a rigorous inversion center in the solid state, its ν(NN) vibration is expected to be very weak and is not discernable in the recorded IR spectra. Additional evidence for the presence of the hydride ligands was gained by treatment of **3** with two equiv of methyl triflate, which led to the formation of methane in 97% yield as measured by gas chromatography (GC).

Dinuclear **3** populates a low-spin singlet ground state, manifiested in its RT ^{1}H NMR spectrum (see the Supporting Information), presumably due to antiferromagnetic exchange between two S = 1/2 centers. This scenario contrasts that of a related diiron(I) linear-N_2-bridged system supported by tris(phosphine)borate ligands ({[PhBP$_3$]Fe}$_2$(μ-N_2)), where the ground spin state is instead S = 3 from weak ferromagnetic coupling between two S = 3/2 centers.[43] The local low-spin environment of each iron center in **3** derives from the presence of a strong-field hydride ligand and its five-coordinate environment. The Fe–P distances in **3** are notably shorter (Fe–P$_{avg}$ 2.16 Å) than those in high-spin {[PhBP$_3$]Fe}$_2$-(μ-N_2) (ranging from 2.34 to 2.39 Å), reflecting its low-spin iron centers.

Whereas the 80 K solid-state Mössbauer spectrum of **3** in a parallel magnetic field (50 mT) shows only one quadrupole doublet (δ = 0.15 mm s^{-1} and ΔE_Q = 0.78 mm s^{-1}), consistent with a single S = 0 species (Figure 3b), a Mössbauer spectrum of **3** obtained as a 2-MeTHF glass instead shows the clear presence of two distinct quadrupole doublets in approximately a 95:5 ratio. The major component is fit satisfactorily with parameters for **3** (δ = 0.15 mm s^{-1} and ΔE_Q = 0.80 mm s^{-1}). The minor component is fit with the parameters δ = 0.34 mm s^{-1} and ΔE_Q = 2.25 mm s^{-1}, similar to S = 1/2 phosphine–iron compounds we have previously characterized[20] (Figure 3c). The 77 K X-band EPR spectrum of **3** in 2-MeTHF confirms the presence of a Kramer's doublet signal, consistent with the presence of a low-spin S = 1/2 species [$P_2^{P'Ph}$Fe(N_2)(H)] (Figure 3 d). These data suggest that, in solution

under nitrogen, dinuclear **3** partially dissociates into two [$P_2^{P'Ph}Fe(N_2)(H)$] species, **4** (Scheme 2).

To confirm the identity of the minor $S = 1/2$ solution component **4**, we performed Q-band (33.7 GHz) Davies ENDOR on 2-Me-THF solutions of both **3** and the isotopologue **3-D** (see the Supporting Information). This study confirms the presence of two ^{31}P nuclei with similar hyperfine couplings ($^{31}P1$ A = [70 70 62] MHz, $^{31}P2$ A = [76 76 66] MHz) in addition to a third, more strongly coupled ^{31}P nucleus ($^{31}P3$ A = [142 144 158] MHz). A large ^{1}H coupling (^{1}H A = [18 64 52] MHz), consistent with a metal-bound hydride, is observed in the natural abundance sample and is of greatly reduced intensity in the sample containing the **4-D** isotopologue. Davies ENDOR was also acquired using pulse parameters optimized for detection of deuterium hyperfine couplings, and here only the **4-D** sample shows ^{2}H ENDOR signals from a bound deuteride, which are well simulated by simply scaling the ^{1}H hyperfine values for the hydride by the gyromagnetic ratios of ^{2}H and ^{1}H ($\gamma = g_n(^2H)/g_n(^1H) = 0.1535$). The X-band CW EPR (Figure 3d) and Q-band electron spin-echo detected EPR (ESE-EPR) (see the Supporting Information) of **4** and **4-D** in 2-Me-THF are well-simulated using the ^{31}P, ^{1}H and ^{2}H hyperfine values determined from the ENDOR spectra with g = [2.0980 2.0900 2.0019].

Using $HBAr^F_4$ as the acid and KC_8 as the reductant, [$P_2^{P'Ph}Fe(H)]_2(\mu\text{-}N_2)$ catalyzed the reduction of N_2 to NH_3 at −78 °C in Et_2O and achieved turnovers of 7.5 ± 0.8 equiv of NH_3s per complex in the presence of 300 equiv acid and 360 equiv reductant (150 and 180 equiv per Fe, respectively; Table 1, entry 1). Allowing the reaction to stir longer did not lead to an increase in yield (entry 2). These results establish catalytic turnover for this new iron catalyst system; its efficiency is not as high as for the $P_3^BFe(N_2)^-$ catalyst, where the presence of substantially less acid/reductant was needed to achieve a similar amount of NH_3. We wondered whether light might improve the yield of ammonia, and employed a Hg lamp to test this possibility. We reasoned that photolysis during catalysis might enhance the break-up of [$P_2^{P'Ph}Fe(H)]_2(\mu\text{-}N_2)$ to a more catalytically active state, for example the [$P_2^{P'Ph}Fe(N_2)(H)$] monomer discussed above, and/or might cause H_2 elimination from less active states, such as the dihydride complex $P_2^{P'Ph}Fe(N_2)(H)_2$ **5** that is discussed below. We were gratified to observe that significantly more ammonia was formed (18.1 ± 0.8 equiv NH_3; ca. 140% improvement in overall yield at the same loading) under Hg lamp photolysis conditions (entry 3). When the reaction was performed with the $P_2^{P'Ph}$ ligand and no Fe (entries 4 and 5), no NH_3 was detected regardless of whether mercury lamp photolysis was applied. The effect of photolysis was more pronounced at higher loadings of $HBAr^F_4$ and KC_8; 3000 equiv acid and 3600 equiv reductant led to 66.7 ± 4.4 equiv NH_3 generated, compared to only 24.5 ± 1.2 equivalents in the absence of photolysis (entries 7 and 8). This correlates to a circa 180% improvement in NH_3 yield in the presence of mercury lamp irradiation.

To discern what types of iron species might be formed under conditions relevant to the overall catalysis, an analysis of the Fe-containing products after **3** was exposed to 10 equiv of acid and 12 equiv of reductant was undertaken and revealed the formation of the dihydride $P_2^{P'Ph}Fe(N_2)(H)_2$ **5** (93% yield based on ^{31}P integration) by NMR and IR spectroscopies (Scheme 2). The data for **5** show a strong N_2 vibration at 2071 cm^{-1} (IR) and

two hydride resonances in the ^{1}H NMR spectrum at δ = −8.87 and −20.5 ppm in C_6D_6. The presence of two phosphine resonances in the ^{31}P NMR spectrum (δ = 119 and 110 ppm) indicate that the $^{i}Pr_2P$ donors are related by symmetry. A structure consistent with these data features a hydride ligand that bisects the two $^{i}Pr_2P$-donors, *trans* to the N_2 ligand, and another hydride ligand *trans* to the central phosphine donor of the chelated tris(phosphine) ligand. The conversion of **3** into **5** can be rationalized by the presence of proton and electron equivalents under N_2 as **3** and two equiv of **5** differ by two H-atoms, along with binding of an additional equiv of N_2. A plausible pathway for this conversion includes the reduction of **3** to two equiv of anionic $[P_2^{P'Ph}Fe(N_2)(H)]^-$ in the presence of excess KC_8. Protonation of this anion would lead to **5** (see the Supporting Information for generation of $[P_2^{P'Ph}Fe(N_2)(H)]^-$ from **3** by KC_8).

Dihydride **5** can be independently synthesized and characterized in solution. Exposure of a degassed THF solution of **3** to H_2, followed by re-exposure to N_2, provides **5** in good yield, as determined by NMR spectroscopy. The 80 K Mössbauer spectrum of a 2-MeTHF solution of **5** shows one quadrupole doublet with parameters δ = 0.05 mm s^{-1} and ΔE_Q = 0.45 mm s^{-1} (see the Supporting Information). When **5** was subjected to the catalytic conditions (150 equiv of $HBAr^F_4$ and 180 equiv of KC_8), 2.6 ± 0.1 equiv of ammonia were detected (entry 9). A greater than 3-fold increase in yield (8.9 ± 0.9 equiv NH_3) was observed when the catalysis was instead performed in the presence of Hg-lamp irradiation (entry 10), suggesting that light-induced H_2 elimination may expose a more catalytically active state of the system, for example by liberating "$P_2^{P'Ph}Fe^0(N_2)$".

To probe whether light might facilitate the break-up of $[P_2^{P'Ph}Fe(H)]_2(\mu\text{-}N_2)$ **3** to monomeric $[P_2^{P'Ph}Fe(N_2)(H)]$ **4**, a THF solution of **3** was exposed to Hg lamp photolysis at −78 °C in an EPR tube. After 10 minutes of photolysis, the tube was freeze-quenched at 77 K and its X-band EPR spectrum was acquired. The intensity of the $S = 1/2$ signal increased, but by a barely discernable amount over time (see the Supporting Information). Given that there is appreciable break-up of **3** to **4** in solution under N_2 in the absence of photolysis (see below), a photodissociation pathway of **3** (Scheme 3) seems unlikely to be the source of the enhanced NH_3 yields under photolysis given how little the signal of **4** increases under irradiation. Given the propensity of $Fe(H)_2$ species to undergo photoinduced reductive elimination of H_2 (for example, Scheme 1) we also subjected a yellow [D_8]toluene solution of purified dihydride **5** in an NMR tube to Hg lamp photolysis. After 1 hour of photolysis, the yellow solution color of **5** had undergone a marked color change to deep red (see the Supporting Information for a comparison), demonstrating appreciable photoinstability. While we do not know the photogenerated products, we speculate "$P_2^{P'Ph}Fe^0(N_2)$" is one plausible candidate (Scheme 3).

A similar experiment using the aforementioned hydride/borohydride complex $(P_3^B)(\mu\text{-}H)Fe(N_2)(H)$, observed during catalysis by $P_3^BFe(N_2)^-$ by freeze-quenched Mössbauer studies,[20] provided more tractable spectroscopic results. Thus, a [D_8]toluene solution of $(P_3^B)(\mu\text{-}H)Fe(N_2)(H)$ was subjected to mercury lamp photolysis at −78 °C in an NMR tube, leading to the formation of $P_3^BFe(N_2)$ and $(P_3^B)(\mu\text{-}H)Fe(H_2)\text{-}(H)$, as discerned by ^{1}H NMR spectroscopy (Figure 4). This observation can be explained as follows: Reductive elimination of H_2 from $(P_3^B)(\mu\text{-}H)Fe(N_2)(H)$ can form $P_3^BFe(N_2)$. Remaining $(P_3^B)(\mu\text{-}$

H)Fe(N_2)(H) may then undergo H_2 for N_2 substitution to generate known (P_3^B)(μ-H)Fe(H_2)(H). These observations suggest that an irradiation strategy may also lead to increased NH_3 catalysis efficiency by $P_3^B Fe(N_2)^-$. Accordingly, at high acid and reductant loadings, a substantial increase in the equivalents of ammonia was observed, with up to 94 equiv of ammonia being detected (88.1 ± 8.0 with light versus 60.0 ± 3.7 with no light, entries 11 and 12).

In conclusion, we have synthesized and structurally characterized a new diiron(I) $[P_2^{P'Ph}Fe(H)]_2(\mu\text{-}N_2)$ complex that is active for catalytic N_2-to-NH_3 conversion. This species partially breaks up into an $S = 1/2$ $[P_2^{P'Ph}Fe(N_2)(H)]$ species in solution under N_2, as established by Mössbauer, EPR, and ENDOR spectroscopies. A monomeric dihydride complex, $P_2^{P'Ph}Fe(N_2)(H)_2$, forms under conditions that model the catalysis, and its N_2-to-NH_3 conversion activity is also enhanced under photolysis, consistent with its observed photoinstability. These observations lead us to speculate that photoinduced release of H_2 is beneficial to the catalysis, perhaps via generation of "$P_2^{P'Ph}Fe^0(N_2)$". While mechanistic studies are needed to further explore this hypothesis, the previously reported $P_3^B Fe(N_2)^-$ system, where an off-path (P_3^B)(μ-H)Fe(N_2)(H) species appears to limit catalytic efficiency, also shows enhanced NH_3 yields under irradiation. Accordingly, irradiation of (P_3^B)(μ-H)Fe(N_2)(H) generates (in part) previously characterized (P_3^B)$Fe^0(N_2)$.

The $[P_2^{P'Ph}Fe(H)]_2(\mu\text{-}N_2)$ system described herein expands on the few well-defined iron systems that mediate catalytic nitrogen fixation against a backdrop of many related iron complexes that have not shown catalytic efficacy under the conditions discussed herein.[17] Dinuclear $[P_2^{P'Ph}Fe(H)]_2(\mu\text{-}N_2)$ differs from tetradentate $P_3^E Fe$ catalysts,[17, 20] and also a recently reported bis(phosphine)pyrrole system, through its use of a trisphosphine donor auxiliary that does not present other heteroatom donors to the iron center.[15] In this context, Ashley and co-workers have recently reported an iron system supported by only phosphine donors that is selective for N_2-to-hydrazine conversion;[44] the present $[P_2^{P'Ph}Fe(H)]_2(\mu\text{-}N_2)$ system does not generate catalytic quantities of hydrazine under the conditions employed here, or with Ashley's reported conditions (see the Supporting Information). The factors that control the N_2-fixing abilities and product profiles of these various iron systems are rich and present a fascinating topic for comparative studies.

Supplementary Material

Refer to Web version on PubMed Central for supplementary material.

Acknowledgments

This work was supported by the NIH (GM070757 and a Ruth L. Kirschstein NRSA Predoctoral Fellowship to Promote Diversity in Health-Related Research to T.M.B.), and the NSF via its MRI program (NSF-1531940). We thank Lawrence Henling and Michael Takase for assistance with XRD studies, Javier Fajardo, Jr., Matthew Chalkley, and Niklas Thompson for insightful discussions, and Dr. Shabnam Hematian for assistance with GC experiments.

References

1. Howard JB, Rees DC. Chem. Rev. 1996; 96:2965–2982. [PubMed: 11848848]
2. Burgess BK, Lowe DJ. Chem. Rev. 1996; 96:2983–3012. [PubMed: 11848849]

3. Hoffman BM, Lukoyanov D, Yang Z-Y, Dean DR, Seefeldt LC. Chem. Rev. 2014; 114:4041–4062. [PubMed: 24467365]
4. Yoo SJ, Angove HC, Papaefthymiou V, Burgess BK, Münck E. J. Am. Chem. Soc. 2000; 122:4926–4936.
5. Einsle O, Tezcan FA, Andrade SLA, Schmid B, Yoshida M, Howard JB, Rees DC. Science. 2002; 297:1696–1700. [PubMed: 12215645]
6. Spatzal T, Aksoyoglu M, Zhang L, Andrade SLA, Schleicher E, Weber S, Rees DC, Einsle O. Science. 2011; 334:940. [PubMed: 22096190]
7. Hoffman BM, Lukoyanov D, Dean DR, Seefeldt LC. Acc. Chem. Res. 2013; 46:587–595. [PubMed: 23289741]
8. Kowalska J, DeBeer S. Biochim. Biophys. Acta Mol. Cell Res. 2015; 1853:1406–1415.
9. a) Siegbahn PEM, Westerberg J, Svensson M, Crabtree RH. J. Phys. Chem. B. 1998; 102:1615–1623.b) Dance I. Dalton Trans. 2010; 39:2972–2983. [PubMed: 20221528] c) Smith D, Danyal K, Raugei S, Seefeldt LC. Biochemistry. 2014; 53:2278–2285. [PubMed: 24654842] d) Siegbahn PEM. J. Am. Chem. Soc. 2016; 138:10485–10495. [PubMed: 27454704]
10. Bazhenova TA, Shilov AE. Coord. Chem. Rev. 1995; 144:69–145.
11. Yandulov DV, Schrock RR. Science. 2003; 301:76–78. [PubMed: 12843387]
12. Ritleng V, Yandulov DV, Weare W, Schrock RR, Hock AS, Davis WM. J. Am. Chem. Soc. 2004; 126:6150–6163. [PubMed: 15137780]
13. Arashiba K, Miyake Y, Nishibayashi Y. Nat. Chem. 2011; 3:120–125. [PubMed: 21258384]
14. Arashiba K, Kinoshita E, Kuriyama S, Eizawa A, Nakajima K, Tanaka H, Yoshizawa K, Nishibayashi Y. J. Am. Chem. Soc. 2015; 137:5666–5669. [PubMed: 25879994]
15. Shogo K, Arashiba K, Nakajima K, Matsuo Y, Tanaka H, Ishii K, Yoshizawa K, Nishibayashi Y. Nat. Commun. 2016; 7:12181–12189. [PubMed: 27435503]
16. Kuriyama S, Arashiba K, Tanaka H, Matsuo Y, Nakajima K, Yoshizawa K, Nishibayashi Y. Angew. Chem. Int. Ed. 2016; 55:14291–14295. *Angew. Chem.* **2016**, *128*, 14503 – 14507.
17. Anderson JS, Rittle J, Peters JC. Nature. 2013; 501:84–87. [PubMed: 24005414]
18. Ung G, Peters JC. Angew. Chem. Int. Ed. 2015; 54:532–535. *Angew. Chem.* **2015**, *127*, 542 – 545.
19. Del Castillo TJ, Thompson NB, Suess DL, Ung G, Peters JC. Inorg. Chem. 2015; 137:7803–7809.
20. Del Castillo TJ, Thompson NB, Peters JC. J. Am. Chem. Soc. 2016; 138:5341–5350. [PubMed: 27026402]
21. Lowe DJ, Thorneley RNF. Biochem. J. 1984; 224:877–886. [PubMed: 6395861]
22. Ertl G. J. Vac. Sci. Technol. A. 1983; 1:1247–1253.
23. Leigh GJ, Jimenez-Tenorio M. J. Am. Chem. Soc. 1991; 113:5862–5863.
24. Komiya S, Akita M, Yoza A, Kasuga N, Fukuoka A, Kai Y. J. Chem. Soc., Chem. Commun. 1993:787–788.
25. Crossland JL, Tyler DR. Coord. Chem. Rev. 2010; 254:1883–1894.
26. Field LC, Hazari N, Li HL. Inorg. Chem. 2015; 54:4768–4776. [PubMed: 25945866]
27. McWilliams SF, Holland PL. Acc. Chem. Res. 2015; 48:2059–2065. [PubMed: 26099821]
28. Lee Y, Mankad NP, Peters JC. Nat. Chem. 2010; 2:558–565. [PubMed: 20571574]
29. Moret M-E, Peters JC. J. Am. Chem. Soc. 2011; 133:18118–18121. [PubMed: 22008018]
30. Anderson JS, Moret M-E, Peters JC. J. Am. Chem. Soc. 2013; 135:534–537. [PubMed: 23259776]
31. Creutz SE, Peters JC. J. Am. Chem. Soc. 2014; 136:1105–1115. [PubMed: 24350667]
32. Chalkley MJ, Del Castillo TJ, Matson BD, Roddy JR, Peters JC. ACS Cent. Sci. 2017; 3:217–223. [PubMed: 28386599]
33. Igarashi RY, Laryukhin M, Dos Santos PC, Lee H-I, Dean DR, Seefeldt LC, Hoffman BM. J. Am. Chem. Soc. 2005; 127:6231–6241. [PubMed: 15853328]
34. Simpson FB, Burris RH. Science. 1984; 224:1095–1097. [PubMed: 6585956]
35. a) Lukoyanov D, Khadka N, Yang Z-Y, Dean DR, Seefeldt LC, Hoffman BM. J. Am. Chem. Soc. 2016; 138:10674–10683. [PubMed: 27529724] b) Lukoyanov D, Khadka N, Yang Z-Y, Dean DR, Seefeldt LC, Hoffman BM. J. Am. Chem. Soc. 2016; 138:1320–1327. [PubMed: 26788586]

36. Sacco A, Aresta M. Chem. Commun. 1968:1223–1224.
37. Aresta M, Giannoccaro P, Rossi M, Sacco A. Inorg. Chim. Acta. 1971; 5:115–118.
38. Whittlesey MK, Mawby RJ, Osman R, Perutz RN, Field LD, Wilkinson MP, George MW. J. Am. Chem. Soc. 1993; 115:8627–8637.
39. Van Der Sluys LS, Eckert J, Eisenstein O, Hall JH, Huffman JC, Jackson SA, Koetzle TF, Kubas GJ, Vergamini PJ, Caulton KG. J. Am. Chem. Soc. 1990; 112:4831–4841.
40. Ballmann J, Munha RF, Fryzuk MD. Chem. Commun. 2010; 46:1013–1025.
41. Mankad NP, Rivard E, Harkins SB, Peters JC. J. Am. Chem. Soc. 2005; 127:16032–16033. [PubMed: 16287283]
42. Addison AW, Rao TN, Reedijk J, van Rijn J, Verschoor GC. J. Chem. Soc., Dalton Trans. 1984:1349–1356.
43. Betley TA, Peters JC. J. Am. Chem. Soc. 2004; 126:6252–6254. [PubMed: 15149221]
44. Hill PJ, Doyle LR, Crawford AD, Myers WK, Ashley AE. J. Am. Chem. Soc. 2016; 138:13521–13524. [PubMed: 27700079]
45. CCDC 1521910 (**2-FeBr$_2$**) and 1521909 (**3**) contain the supplementary crystallographic data for this paper. These data are provided free of charge by The Cambridge Crystallographic Data Centre.
46. Experimental conditions: microwave frequency = 9.409 GHz; microwave power = 6.423 mW; modulation frequency = 100 kHz; modulation amplitude = 1 G; conversion time = 82 ms; time constant = 20.5 ms; temperature = 77 K. Simulation parameters: g = [2.0980 2.0900 2.0019]; ^{31}P1 A = [70 70 62] MHz, colinear with g; ^{31}P2 A = [76 76 66] MHz, colinear with g; ^{31}P3 A = [142 144 158] MHz, Euler angle β of 20° relative to g tensor; Hydride ^{1}HA = [18 64 52] MHz, Euler angle β of 20° relative to g tensor, Deuteride ^{2}H A = ^{1}H A*(g_n(^{2}H)/g_n (^{1}H)) = [2.8 9.8 8.0] MHz.

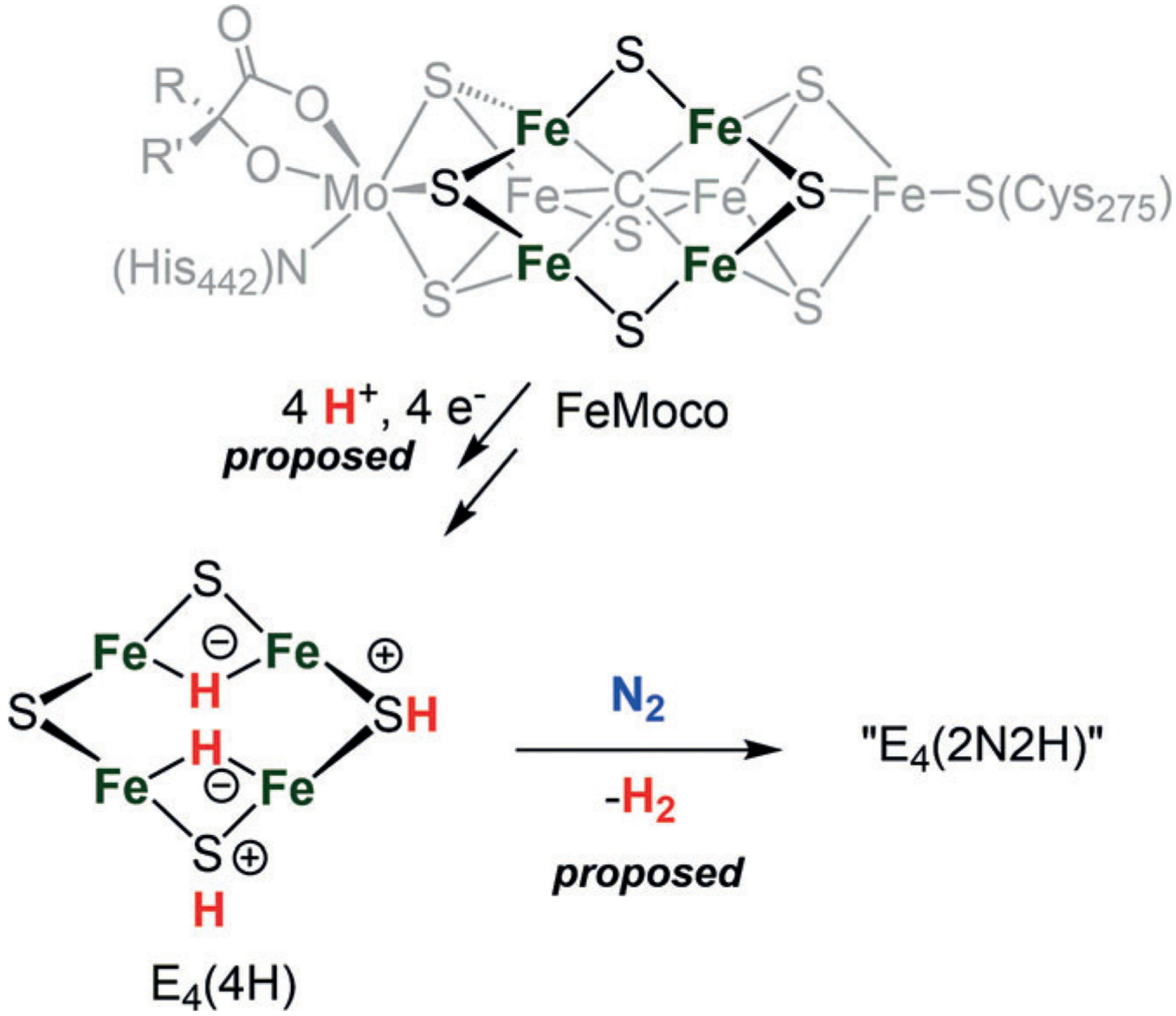

Figure 1.

Top: The FeMoco active site of MoFe-nitrogenase.[6] Bottom: Conversion of a proposed $E_4(4\ H)$ intermediate state of FeMoco into an activated E_4 state with N_2 bound.[21]

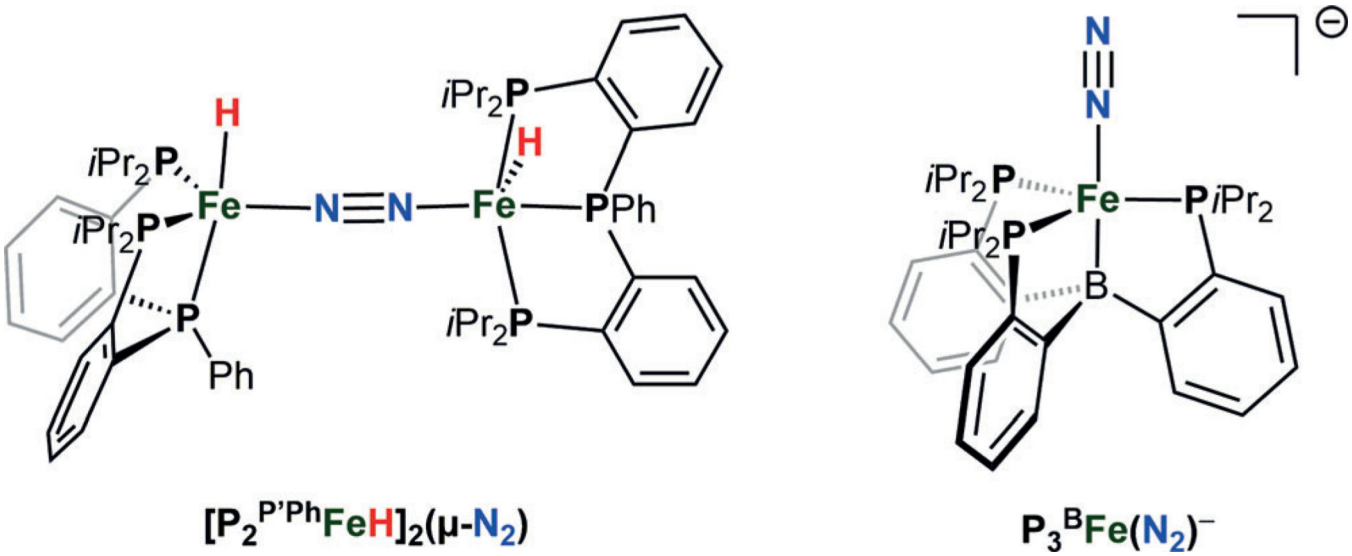

Figure 2.

The new diiron(I)–μ-N_2 catalyst (left) and previously reported $P_3{}^BFe(N_2)^-$ (right) that provide higher yields of ammonia under Hg lamp photolysis.

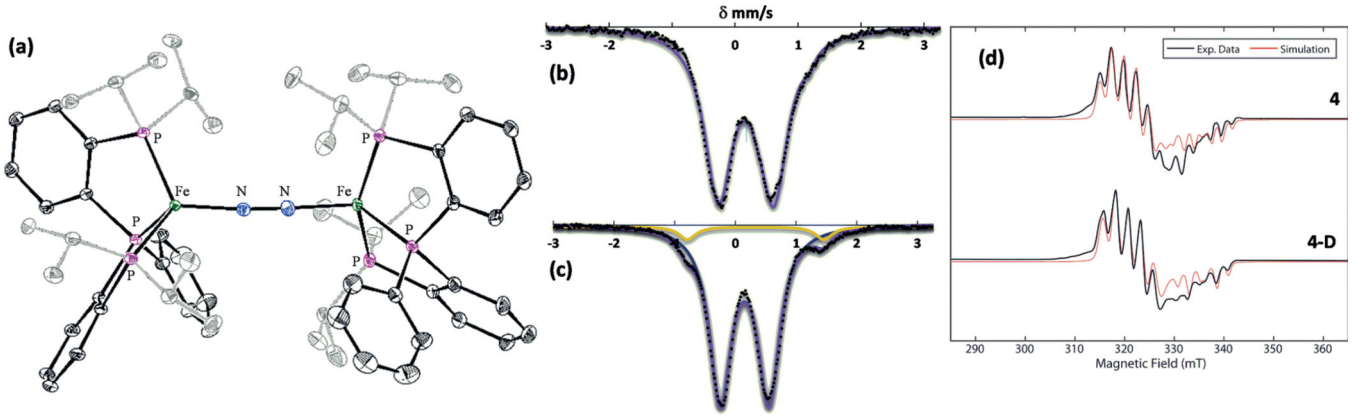

Figure 3.

a) X-ray structure of **3** with ellipsoids set at 50% probability (solvent and second dinuclear Fe molecule not shown; minor component of disordered isopropyl groups omitted for clarity).[45] b) The 80 K, 50 mT, solid-state ^{57}Fe Mössbauer spectrum of **3**. Data: black points, simulation: purple line. c) The 80 K, 50 mT, ^{57}Fe Mössbauer spectrum of a 2-MeTHF solution of **3**. Major $S = 0$ component: blue, minor $S = 1/2$ component: yellow. d) X-band Continuous Wave (CW) EPR spectra (black) of **4** (top trace) and **4-D** (bottom trace) in 2-Me-THF with simulations of each (red).[46]

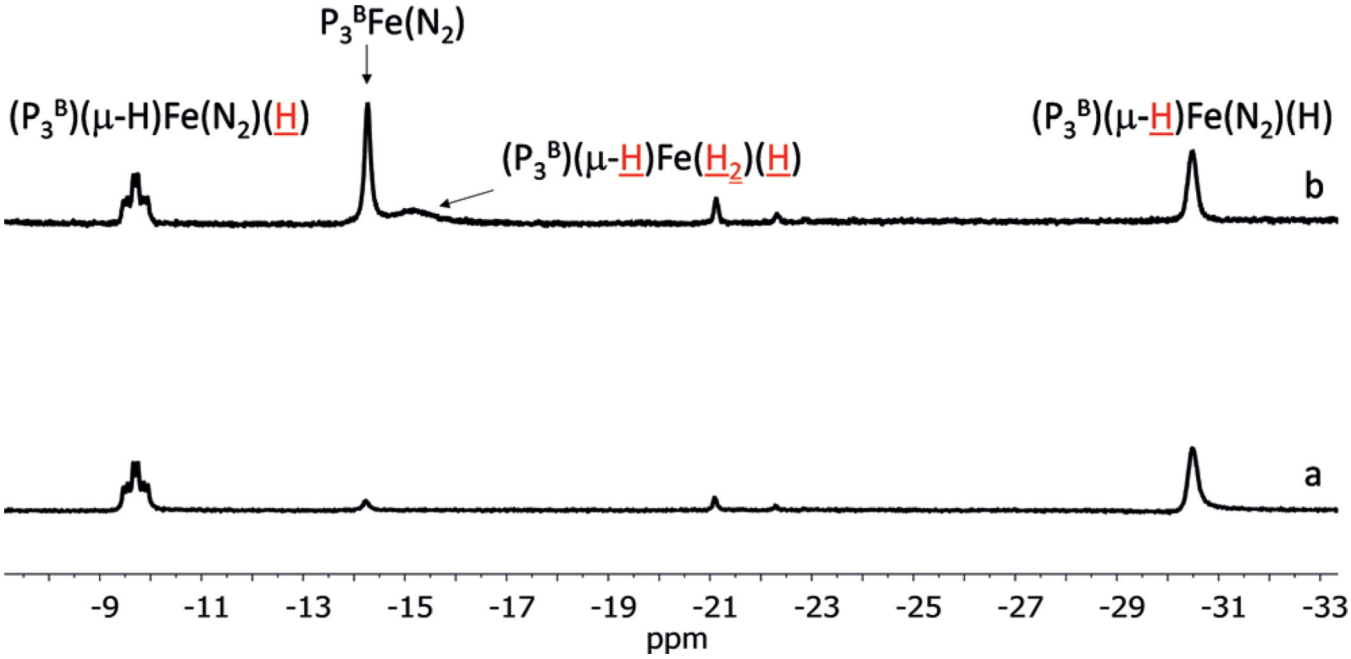

Figure 4.

Hydride region of ^{1}H NMR spectrum of a [D_8]toluene solution of (P_3^B)(μ-H)Fe(N_2)(H) pre-photolysis (spectrum a) and after 10 minutes of Hg lamp photolysis at −78°C (spectrum b). The proton-(s) corresponding to the ^{1}H resonance are depicted in red and are underlined.

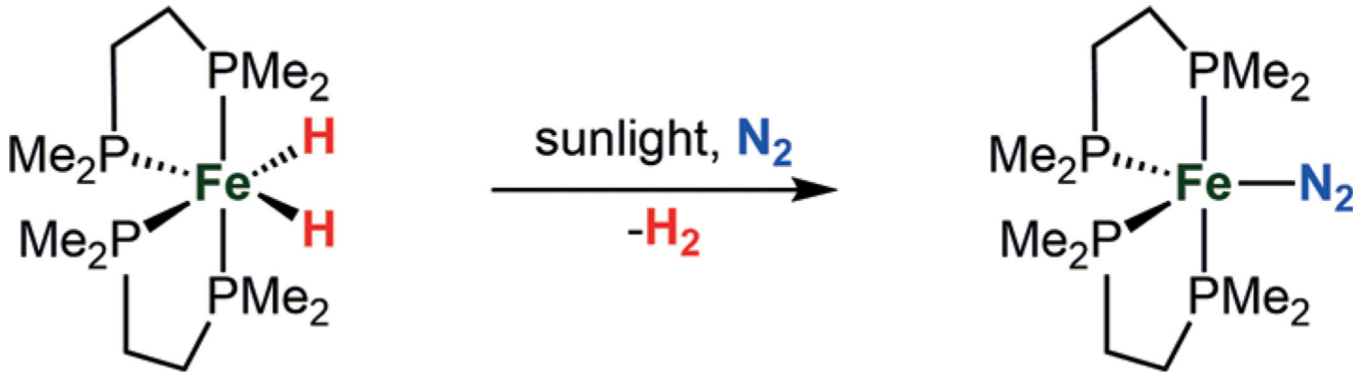

Scheme 1.

Reductive elimination of H_2 from a polyphosphine iron complex in the presence of N_2 and sunlight, leading to an activated Fe(N_2) complex.[36–39]

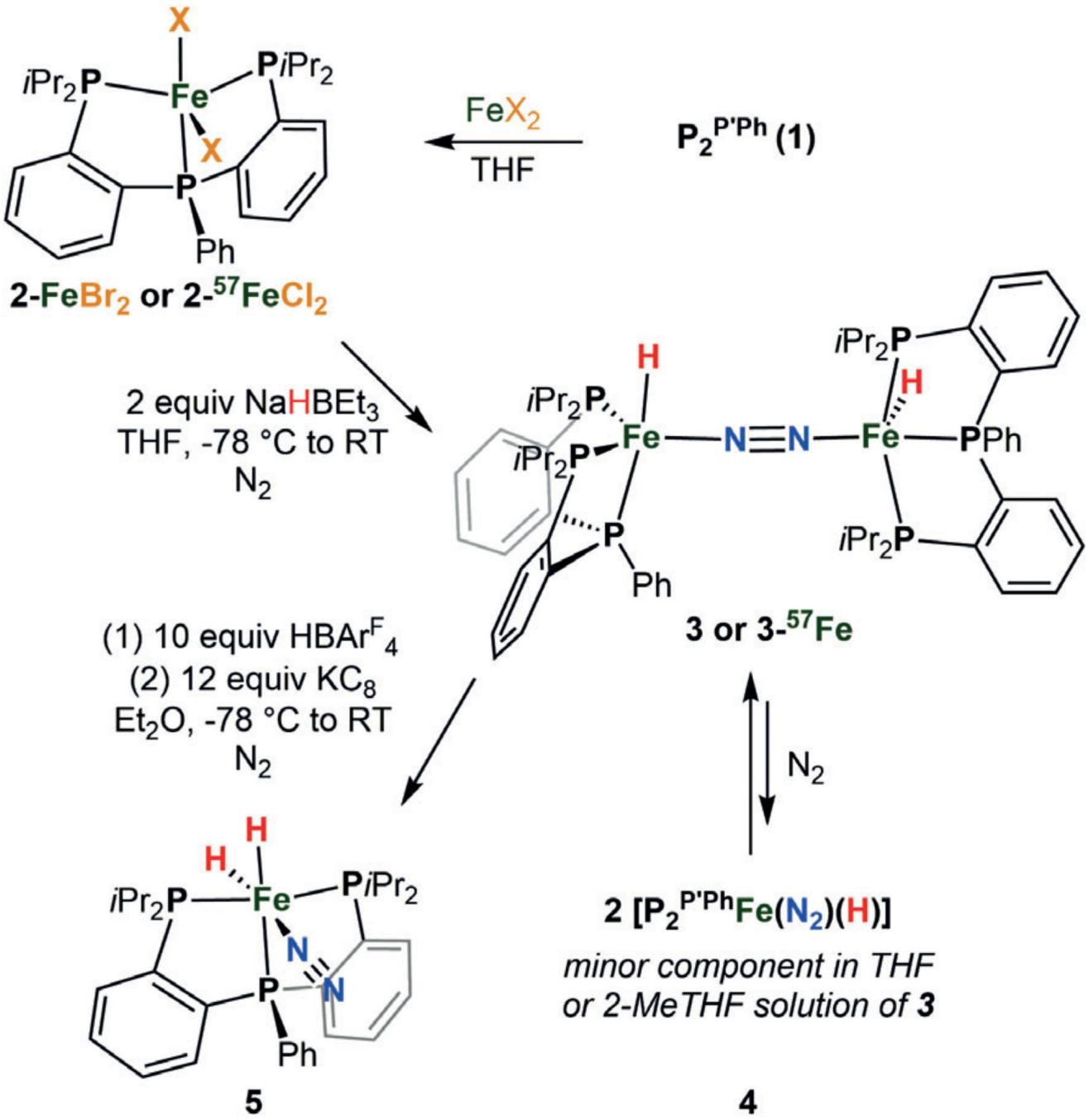

Scheme 2.
Synthesis of Fe complexes discussed herein.

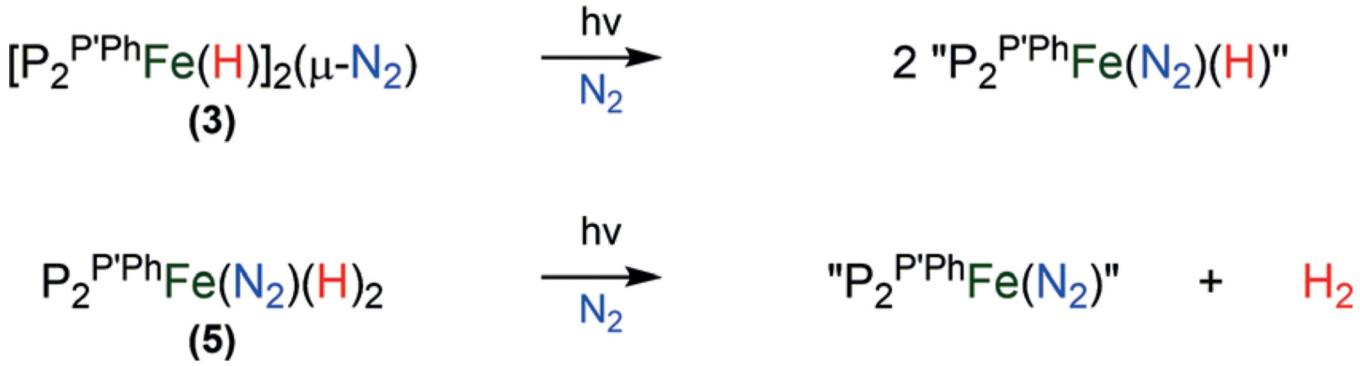

Scheme 3.

Possible roles for light in catalysis: photodissociation of dinuclear **3** to a monomer and/or reductive elimination of H_2 from an $Fe(H)_2$ complex **5**.

Table 1

Catalytic dinitrogen reduction to ammonia with synthetic Fe complexes.[a]

	Variation	$HBAr^F_4$ (equiv)	KC_8 (equiv)	Mean ± SD (equiv NH_3)
1		300	360	7.5 ± 0.8
2[b]	overnight	300	360	8.7 ± 0.7
3	Hg Lamp	300	360	18.1 ± 0.8
4[b]	$P_2^{p'Ph}$, no Fe	150	180	< 0.1
5[b]	$P_2^{p'Ph}$, no Fe, Hg lamp	150	180	< 0.1
6[b]	2-MeTHF instead of Et_2O	300	360	0.5 ± 0.3
7		3000	3600	24.5 ± 1.2
8	Hg Lamp	3000	3600	66.7 ± 4.4
9[b]	**5** instead of **3**	150	180	2.6 ± 0.1
10[b]	**5** instead of **3**, Hg lamp	150	180	8.9 ± 0.9
11	$P_3^BFe(N_2)^-$ instead of **3**	1500	1800	60.0 ± 3.7
12	$P_3^BFe(N_2)^-$ instead of **3**, Hg lamp	1500	1800	88.1 ± 8.0

[a] All entries are an average of 3 runs unless otherwise noted.

[b] Average of 2 runs. Note: Ammonia yields are reported per complex.